High-strength high-surface-area porous carbon made from submicron-diameter carbon filaments

XIAOPING SHUI and D.D.L. CHUNG
Composite Materials Research Laboratory, State University of New York at Buffalo
Buffalo, NY 14260-4400

(Received 4 January 1996; accepted in revised form 9 April 1996)

Keywords: porous carbon, carbon filaments, carbon fibers, strength, surface area, electrical resistivity.

Porous carbons with porosity above 50 vol.% are useful for numerous non-structural applications, such as electrodes, catalysts, catalyst support, filters, chemical absorbers, molecular sieves, membranes, dental and surgical prosthetic devices and thermal insulators [1-14]. These carbons can be made from carbon fibers, which may be bound by a binder such as a polymer, pitch or carbon. Alternatively they can be made by carbonizing organic fibers that are bound by a binder. In either case, a pore forming agent may be used, although it is not essential. Porous carbons can also be made from a polymer (such as a phenolic) that is not in the form of fibers, through foaming and carbonization. Due to the large diameter (typically 10 μm or more) of the carbon or organic fibers for the fiber-based porous carbons and due to the foaming process for the polymer-based porous carbons, the pores in the resulting porous carbons are large (> 40 μm in mean size). As a result, the porous carbons are low in strength (< 7 MPa under compression) and in the specific geometric surface area (SGSA, <1,100 cm^2/cm^3). This problem is more serious for the polymer-based porous carbons than the fiber-based porous carbons. In this work, by using submicron diameter carbon filaments in place of carbon fibers (typically 10 μm in diameter), we obtained a porous carbon of mean pore size 4 μm, SGSA 35,000 cm^2/cm^3 and compressive strength 30-35 MPa. For the sake of comparison, fiber-based and phenolic-based porous carbons were also tested. Both filament-based and fiber-based porous carbons used carbon (from pitch) as the binder and were similarly fabricated from discontinuous filaments or fibers, whereas the phenolic-based porous carbon (also known as reticulated vitreous carbon) was supplied by Energy Research and Generation, Inc. (Oakland, CA).

The carbon filaments were of diameter 0.2 μm, length >100 μm and density 2.0 g/cm^3, and were supplied by General Motors Corp. (Warren, Michigan); they were fabricated by catalytic growth from carbonaceous gases. The carbon fibers were of diameter 10 μm, length 50, 100, 200 or 400 μm and density 1.6 g/cm^3, and were supplied by Ashland Petroleum Co. (Ashland, Kentucky); they were fabricated by carbonizing pitch fibers.

Filament-based and fiber-based porous carbons were fabricated using a five step process: (i) carbon filament/fiber slurry preparation, (ii) slurry casting, (iii) baking, (iv) impregnation with pitch, and (v) carbonization. During slurry preparation, the carbon filaments/fibers were dispersed in water containing a surfactant, Triton X-114 (Rohm and Haas Co., Philadelphia, PA). The slurry was poured into a mold, which allowed the excess water to drain. The wet block was removed from the mold and then baked at 85-95°C for 8 h. The dried block (called a preform) was impregnated with pitch dissolved in methylene chloride, and then air dried for a minimum of 24 h. Carbonization of the block was achieved by heating in a nitrogen atmosphere at a rate of 10-20°C/min up to 1000-1200°C, holding for 1 h, and then cooling to room temperature.

Fig. 1 shows SEM photographs of a porous carbon made from carbon filaments. Though the individual filaments in the porous carbon were observed, the binder was distinctly observed as patches in the micrographs. Fig. 2 shows SEM photographs of a porous carbon made from 100 μm long fibers. Bonding by the carbon binder occurs at the fiber junctions. For the sake of comparison, Fig. 3 shows SEM photographs of phenolic-based porous carbons of pore densities 45, 100 and 500 pores per inch (ppi). Except for the 500 ppi porous carbon, all phenolic-based porous carbons exhibit a honeycomb structure. For the 45 ppi (Fig. 3b) and 100 ppi (Fig. 3d) samples, the phenolic based porous carbon's struts are essentially rectangular in their

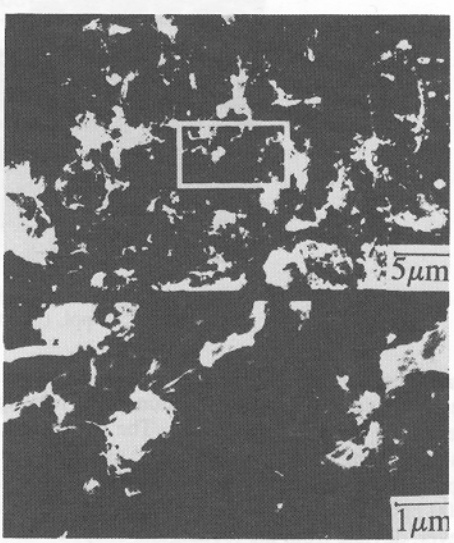

Fig. 1. SEM photographs of filament based porous carbon. The lower photograph is a higher magnification view of the part of the upper photograph inside the rectangle.

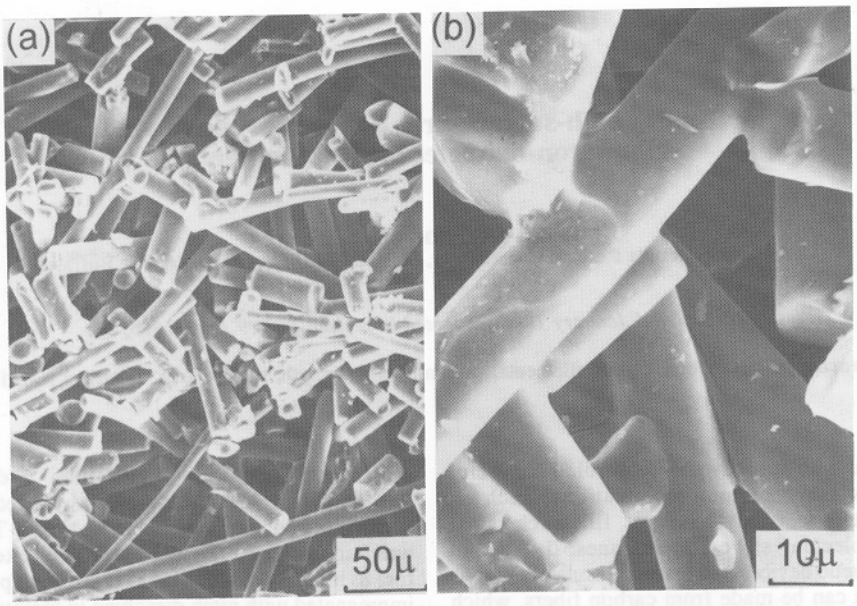

Fig. 2. SEM photographs of fiber based porous carbon made with 100 μm long fibers.

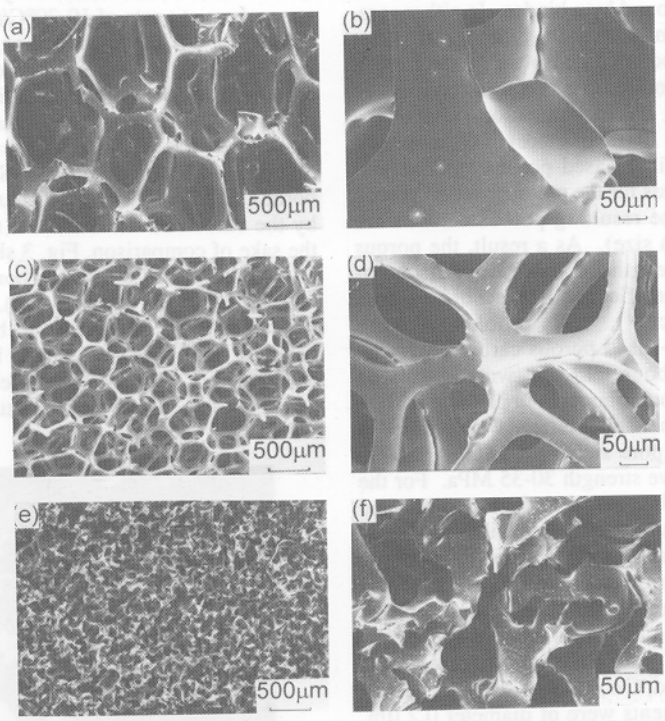

Fig. 3. SEM photographs of phenolic based porous carbons (a) and (b) 45 ppi, (c) and (d) 100 ppi, (e) and (f) 500 ppi.

planar shape, and are relatively smooth and straight, but decrease in width (the narrow portion of the rectangular shape) as the pore size decreases. The strut widths, as measured from SEM photographs, are 190 μm for 30 ppi, 110 μm for 45 ppi, 70 μm for 80 ppi, and 40 μm for 100 ppi. The struts of the 500 ppi (Fig. 3f) sample, however, deviate from the rectangular shape in that they are curved, twisted, and of varied width (average width = 30 μm).

The compressive strength of the porous carbons was measured by applying a force in the transverse direction (defined in Table 1) to a 10 x 10 x 10 mm cube at a crosshead speed of 1 mm/min. The compressive strengths of the 100 ppi and 500 ppi phenolic based porous carbons were impossible to obtain due to their extreme brittleness.

The volume resistivity of the porous carbons was measured using the four-probe method. Each porous carbon was shaped into a rectangular bar with the longest axis being the axis of the resistivity measurement. Silver paint served as the electrical contacts. The volume electrical resistivity (ρ) was determined as a function of

the inner probe separation (l), the cross sectional area of the sample (A), and the potential drop (ΔV) between the inner probes for a known current flow (I) through the bar, using equation (1)

$$\rho = (\Delta V/I)(A/l) \quad (1)$$

In the case of the filament/fiber based porous carbons, volume electrical resistivity measurements were made in two directions, namely the direction parallel to the flow during slurry casting (the transverse direction) and the direction perpendicular to the flow (the longitudinal direction). For the phenolic based porous carbons, the longitudinal direction corresponded to the direction parallel to the planar surface of the sample, whereas the direction perpendicular to the planar surface (i.e., through the sample thickness) corresponded to the transverse direction.

The apparent density of the porous carbon was determined by dividing the weight of a sample by its dimensions. The sample dimensions were measured using a micrometer.

The equation used to determine the specific geometric surface area (SGSA) of the porous carbons was derived from the filament, fiber or strut surface area and the porous carbon volume. For the filament/fiber based porous carbons,

$$SGSA = S_f/V_t \quad (2)$$

where

S_f = surface area of the filament/fiber, and
V_t = total volume of the porous carbon.

However,

$$V_f/V_t = \delta_{app}/\delta_f \quad (3)$$

where

V_f = volume of the filament/fiber,
δ_{app} = apparent density, and
δ_f = density of the filament/fiber.

Therefore, substituting for V_t in equation (2) gives

$$SGSA = (\delta_{app}/\delta_f)(S_f/V_f) \quad (4)$$

Substituting $S_f = 2\pi r\mathcal{L}$, and $V_f = \pi r^2\mathcal{L}$ into equation (4) and simplifying gives

$$SGSA = (\delta_{app}/\delta_f)(2/r) \quad (5)$$

where

r = the radius of the filament/fiber, and
$\mathcal{L}$ = the length of the filament/fiber.

Following the same logic, equation (6), the equivalent of equation (5), was obtained for the phenolic based porous carbon, which has struts of rectangular (dimensions L and w) rather than circular cross-sectional shape.

$$SGSA = 2(\delta_{app}/\delta_s)\{(L+w)/(Lw)\} \quad (6)$$

where

δ_s = density of the strut,
L = length of the strut, and
w = width of the strut.

The porous carbon porosity was given by 1 - (δ_{app}/δ_f) for the filament/fiber-based porous carbon and 1 - (δ_{app}/δ_s) for the phenolic-based porous carbon. The mean pore size was determined from SEM photographs.

Table 1 summarizes the mechanical, electrical and structural properties of the porous carbons studied. Due to the small diameter of the carbon filaments, the filament based porous carbon had a much smaller mean pore size than the fiber-based porous carbons, which in turn had smaller mean pore sizes than almost all of the phenolic based porous carbons. The exceptionally small mean pore size of the filament based porous carbon resulted in exceptionally high compressive strengths in both longitudinal and transverse directions. The small filament diameter also resulted in an exceptionally high SGSA for the filament-based porous carbon. The porosity of the filament based porous carbon was

Table 1. Comparison of porous carbon mechanical, electrical and structural properties.

	Filament based porous carbon	Fiber based porous carbon				Phenolic based porous carbon					
		50 µm long fibers	100 µm long fibers	200 µm long fibers	400 µm long fibers	500 ppi	100 ppi	80 ppi	45 ppi	30 ppi	20 ppi
Apparent density (g/cm^3)	0.7	0.66	0.62	0.43	0.29	0.372	0.107	0.091	0.051	0.047	0.047
Porosity (%)	56.3	58.8	61.3	73.2	81.8	75.0	92.8	94.4	96.8	97.1	97.1
Volume electrical resistivity (Ω.cm)											
longitudinal*	0.017	0.032	0.041	0.060	0.104	-	-	0.467	0.607	0.790	0.682
transverse**	0.12	0.051	0.066	0.102	0.233	-	-	0.545	0.978	0.918	1.810
anisotropy[b]	7.1	1.6	1.6	1.7	2.2	-	-	1.2	1.6	1.2	2.7
Compressive strength (MPa)											
longitudinal*	35	7.7	5.5	2.6	1.6	-	-	-	-	-	-
transverse**	30	6.9 ±0.4	4.8 ±0.3	1.8 ±0.1	0.55 ±0.05	c	c	0.287 ±0.01	0.168 ±0.034	0.113 ±0.018	0.089 ±0.004
Mean pore size (µm)	4	42	50	80	100	75	110	350	750	900	-
Specific geometric surface area (cm^2/cm^3)	35000	1030[a]	968[a]	670[a]	455[a]	10.95	2.17	1.00	0.45	0.21	-

* Perpendicular to direction of flow during slurry casting for the filament/fiber based porous carbons, and in-plane for the phenolic based porous carbons.
** Parallel to direction of flow during slurry casting for the filament/fiber based porous carbon, and through the material thickness for the phenolic based porous carbons.
[a] Calculated from the corresponding apparent density by ignoring the contacts between the fibers and ignoring the tips of the fibers.
[b] Ratio of transverse resistivity to longitudinal resistivity.
[c] Too brittle for testing the compressive strength.

slightly lower than those of the fiber based porous carbons and much lower than those of the phenolic based porous carbons.

The longitudinal electrical resistivity of the filament based porous carbon was lower than those of the fiber based porous carbons, while the transverse resistivity of the filament based porous carbon was within the range exhibited by the fiber based porous carbons. Therefore, the resistivity anisotropy (ratio of transverse resistivity to longitudinal resistivity) was much greater for the filament based porous carbon than the fiber based porous carbons. This implies a greater degree of two-dimensional alignment for the filaments than the fibers. For both filament based and fiber based porous carbons, the transverse resistivity was greater than the longitudinal resistivity, so, for both types of porous carbon, the filaments/fibers were preferentially aligned in the plane perpendicular to the direction of flow during slurry casting. Both longitudinal and transverse resistivities were higher for the phenolic based porous carbons than the filament/fiber based porous carbons.

The technologically attractive properties of the filament based porous carbon compared to the fiber based or phenolic based porous carbons are mainly high compressive strength and high SGSA. These properties are particularly attractive for electrodes, catalyst support, chemical absorbers and prosthetic devices. In addition, the small pore size of the filament based porous carbon makes this porous carbon attractive for certain filters and membranes.

Acknowledgment - This work was supported in part by Amax Foundation, Inc.

REFERENCES

1. E.E. Hucke, U.S. Patent 3,859,421 (1975).
2. J. Wang, *Electrochim. Acta* **26**, 1721 (1981).
3. A.N. Strohl and D.J. Curran, *Anal. Chem.* **51**, 1050 (1979).
4. W.J. Blaedel and J. Wang, *Anal. Chem.* **52**, 76 (1980).
5. I.C. Agarwal, A.M. Rochon, H.D. Gesser and A.B. Sparling, *Water Res.* **18**, 227 (1984).
6. A.P. Sylwester, J.H. Aubert, P.B. Rand, C. Arnold, Jr. and L.R. Clough, *Polym. Mater. Sci. Eng.* **57**, 113 (1987).
7. A.P. Sylwester and R.L. Clough, *Synth. Met.* **29**, F253 (1989).
8. U.S. Patent 4,832,870 (1989).
9. Y. Oren and A. Soffer, *Electrochim. Acta* **28**, 1649 (1983).
10. C. Lestrade, P.Y. Guyomar and M. Astruc, *Environ. Technol. Lett.* **2**, 409 (1981).
11. P.Y. Guyomar, M. Astruc and J.P. Dubreuil, Heavy Met. Environ., Int. Conf., 3rd, 1981, p. 80-83, CEP Consult. Ltd.: Edinburgh, UK.
12. Japanese patent J02053992-A 90.02.22 (9014) JP.
13. Japanese patent J01266222-A 89.10.24 (8948) JP.
14. Japanese patent J02106876-A 90.04.18 (9022) JP.

Mechanical Damage of Carbon Nanotubes by Ultrasound

K.L. Lu
Institute of Chemistry, Academia Sinica, Taipei, Taiwan, Republic of China

R.M. Lago, Y.K. Chen and M.L.H. Green*
The Catalysis Centre, Inorganic Chemistry Laboratory, University of Oxford, South Parks Road, Oxford, OX1 3QR, UK

P.J.F. Harris and S.C. Tsang
The Catalysis Research Centre, Department of Reading, University of Reading, Whiteknights, Reading, UK

(Received 15 April 1996; accepted 22 April 1996)

Keywords: Carbon nanotubes, ultrasound, damage, defects, TEM, ESR, Raman

The discovery of carbon nanotubes by Iijima [1] and the report of their large scale production method by Ebbesen and Ajayan [2] have stimulated a great deal of interest on this new tubular form of carbon. Present evidence suggests that most nanotubes are made up of hollow concentric cylinders of carbon capped at both the tube ends, which is described as a Russian doll model [1].

Dravid et. al. [3], however, suggested an alternative model described as 'paper roll' of which nanotubes are composed of spiral scrolls of graphene sheets. Amelinckx [4] has recently proposed an intermediate case, whereby the nanotubes consist of cylindrical sheets, with scrolls of constant helicity interspersed between them. These models could be virtually indistinguishable when viewed by TEM [5]. Recent discussion shows that nanotubes are structural, flexible and fragile when stress is applied [6-7]. Here we describe the effect of treatment of carbon nanotube samples with high energy ultrasound.

Carbon nanotubes were prepared by the previously described procedure [8]. Samples of the tubes (5 mg) were suspended in 15 mL of CH_2Cl_2 cooled to 0°C and irradiated for 5 to 20 min using a standard horn with a *ca.* 17 W power delivery as estimated by calorimetric measurements [9].

The electron micrographs of the resulting sonicated nanotubes revealed a very high concentration of defects such as bending and buckling (Figure 1a). We note that bent tubes with buckling defects are also occasionally observed in non-sonicated samples. When the duration of the sonication time was increased then the treated tubes showed more defects and more serious damage. Indeed the cavitation process was so energetic

*Author for correspondence